ACS OMEGA

http://pubs.acs.org/journal/acsodf

Article

Design, Synthesis, and Evaluation of a New Series of Hydrazones as Small-Molecule Akt Inhibitors for NSCLC Therapy

Burak Erdönmez, Mehlika Dilek Altıntop,* Gülşen Akalın Çiftçi, Ahmet Özdemir, and Abdulilah Ece

Cite This: *ACS Omega* 2023, 8, 20056−20065

Read Online

ACCESS | Metrics & More | Article Recommendations | Supporting Information

ABSTRACT: In an endeavor to identify small molecules for the management of non-small-cell lung carcinoma, 10 new hydrazone derivatives (**3a**−**j**) were synthesized. MTT test was conducted to examine their cytotoxic activities against human lung adenocarcinoma (A549) and mouse embryonic fibroblast (L929) cells. Compounds **3a**, **3e**, **3g**, and **3i** were determined as selective antitumor agents on A549 cell line. Further studies were conducted to figure out their mode of action. Compounds **3a** and **3g** markedly induced apoptosis in A549 cells. However, both compounds did not show any significant inhibitory effect on Akt. On the other hand, *in vitro* experiments suggest that compounds **3e** and **3i** are potential anti-NSCLC agents acting through Akt inhibition. Furthermore, molecular docking studies revealed a unique binding mode for compound **3i** (the strongest Akt inhibitor in this series), which interacts with both hinge region and acidic pocket of Akt2. However, it is understood that compounds **3a** and **3g** exert their cytotoxic and apoptotic effects on A549 cells *via* different pathway(s).

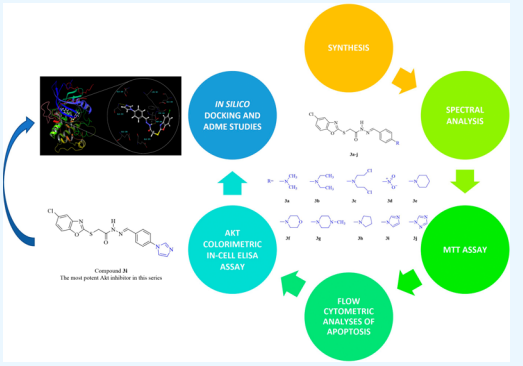

Downloaded via 85.104.48.185 on June 18, 2023 at 17:54:33 (UTC).
See https://pubs.acs.org/sharingguidelines for options on how to legitimately share published articles.

1. INTRODUCTION

Cancer remains a deadly global health concern with more than 200 different types, affecting over 60 human organs.[1] Among all cancers, lung cancer is the primary cause of cancer-related morbidity and mortality in males, while, in females, it ranks second for mortality, after breast cancer, and third for incidence, after breast and colorectal cancer.[2] The disease is notorious for its exceptional potency to spread to distant parts of the body (metastasis), as well as its ability to progress rapidly in its early stages.[3]

There are two groups of lung cancer, namely, small cell lung carcinoma (SCLC) and non-small-cell lung carcinoma (NSCLC).[1] 85% of lung cancer cases are attributed to NSCLC.[4]

Surgery, chemotherapy, radiotherapy, immunotherapy, and targeted therapy are currently available approaches for NSCLC therapy.[5] The best treatment strategy for patients with early-stage NSCLC is still surgical intervention. However, surgery is no longer an option for patients with advanced or metastatic NSCLC.[6,7] Major treatment approaches for unresectable NSCLC are chemotherapy and radiotherapy.[7] Platinum-based chemotherapeutics, taxanes, and other chemotherapeutics (e.g., vinorelbine, gemcitabine, and pemetrexed) are used either alone or in combination.[5] Despite their benefits in NSCLC therapy, these chemotherapeutics damage healthy cells as well as cancer cells and therefore they cause severe adverse effects and toxicity.[8] Resistance to radio(chemo)-therapy is also a significant barrier to NSCLC therapy resulting in tumor recurrence and disease progression.[9] The current challenges in the diagnosis and treatment of NSCLC lead to poor prognosis and low survival rate.[10]

Akt belongs to the family of serine/threonine-specific protein kinases essential for regulating crucial cellular processes including cell survival, proliferation, growth, apoptosis, and glucose metabolism. The abnormal overexpression or activation of Akt is involved in a variety of human malignancies and therefore inhibiting Akt has emerged as a pivotal strategy for the treatment of various types of cancer, particularly B-cell malignancies, NSCLC, and breast cancer.[11−13] Despite the large number of Akt inhibitors developed to date, the U.S. Food and Drug Administration has not approved any Akt inhibitors yet.[11]

Hydrazides-hydrazones are frequently occurring eligible motifs in druglike small molecules due to their distinctive characteristics and several pharmaceutical applications for the treatment of many diseases, particularly severe bacterial infections, cancer, and inflammation.[14−18] Hydrazones have been reported to exert striking antitumor action *via* induction of apoptosis, cell cycle arrest, inhibition of angiogenesis, and a plethora of cancer-related biological targets (e.g., Akt).[19−26]

Received: April 6, 2023
Accepted: May 15, 2023
Published: May 24, 2023



© 2023 The Authors. Published by American Chemical Society

Benzoxazoles are privileged building blocks for the synthesis of biologically active ligands targeting a plethora of crucial targets/pathways due to their unique features allowing them to effectively bind to diverse biological targets with distinct affinities.[27−31] Several studies have revealed that benzoxazoles exert marked cytotoxic activity against a variety of cancer cell lines through diverse mechanisms including induction of apoptosis, inhibition of Akt phosphorylation, and so on.[32−39]

The publications related to hydrazones[19−26] and benzoxazoles[32−39] exerting pronounced anticancer activity through inhibition of target enzymes involved in the pathogenesis of lung cancer motivated us to design novel anti-NSCLC agents by means of the molecular hybridization of the benzoxazole core with the hydrazide group, which was conjugated with the benzylidene moiety substituted at the *para* position with dialkylamino groups (dimethylamino, diethylamino), nitrogen-containing electron-withdrawing groups (nitro substituent), five- (pyrrolidine) or six-membered heterocyclic motifs (piperidine, morpholine and piperazine), heteroaromatic rings (imidazole, triazole) based on our previous work (Figure 1),[21] and the structure−activity relationships of existing Akt inhibitors[11] together with the bioisosteric replacement. In this context, the designed compounds were synthesized readily and assessed for their cytotoxic properties on human lung adenocarcinoma (A549) and mouse embryonic fibroblast (L929) cells. *In vitro* experimental studies were carried out for promising anti-NSCLC agents to shed light on their mechanism of action.

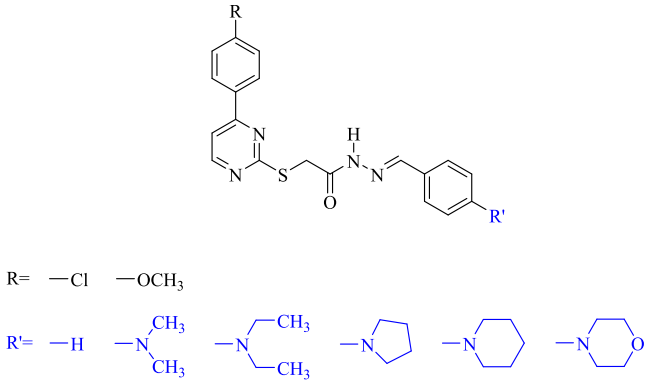

Figure 1. Pyrimidine-based hydrazones reported previously as anticancer agents by our research team.[21]

2. RESULTS AND DISCUSSION

2.1. Chemistry. The hitherto unreported hydrazones (**3a−j**) were prepared as depicted in Scheme 1. The base-catalyzed reaction of 5-chloro-2-mercaptobenzoxazole with ethyl chloroacetate yielded ethyl 2-[(5-chlorobenzoxazol-2-yl)thio]-acetate (**1**), which subsequently underwent a reaction with hydrazine hydrate affording the corresponding hydrazide (**2**). Finally, compound **2** was reacted with 4-substituted benzaldehydes to obtain compounds **3a−j**. Infrared (IR), nuclear magnetic resonance (NMR, ^{1}H and ^{13}C), and high-resolution mass spectrometry (HRMS) were used to verify their chemical structures. These spectra are provided in the Supporting Information.

In the IR spectra of compounds **3a−j**, the N−H stretching band of the hydrazone group was detected at 3207.62−3159.40 cm^{-1}, while the C═O stretching band was detected at 1705.07−1654.92 cm^{-1}. In the ^{1}H NMR spectra of compounds **3a−j**, S-CH$_2$ protons gave rise to two singlets in the range of 4.25−4.73 ppm. The peaks at 11.47−12.09 ppm were attributed to the N−H proton of the hydrazone moiety, while the peaks in the region 7.88−8.26 ppm were assigned to the CH═N proton. In the ^{13}C NMR spectra of compounds **3a−j**, the S-CH$_2$ carbon gave rise to a singlet in the region 34.76−35.02 ppm. The signals due to the CH═N and the C═O carbons were detected in the range of 142.95−145.19 ppm and 167.08−168.27 ppm, respectively. In all HRMS spectra, the predicted and measured m/z values for $[M + H]^+$ were consistent with each other.

2.2. Biochemistry. The hydrazide (**2**) and the hydrazones (**3a−j**) were assessed for their cytotoxic features on A549 human lung adenocarcinoma and L929 mouse embryonic fibroblast cells. The IC$_{50}$ values of the compounds are presented in Table 1. Compounds **3a**, **3e**, **3g**, and **3i** showed cytotoxic effects on A549 cells with IC$_{50}$ values of 91.35 ± 21.89, 176.23 ± 56.50, 46.60 ± 6.15, and 83.59 ± 7.30 μM, respectively. The selectivity index (SI) values of compounds **3a**, **3e**, **3g**, and **3i** were found as >5.47, >2.84, 5.94, and >5.98, respectively. It can be concluded that these agents exert cytotoxic activity against A549 cells without influencing normal (L929) cells at their effective doses.

According to the data presented in Table 1, the replacement of the dimethylamino group (compound **3a**) with the diethylamino substituent (compound **3b**) led to a significant decline in anticancer activity. This outcome indicated that the elongation of the alkyl chains reduced the cytotoxic effect on A549 cells. The bis(2-chloroethyl) and the nitro groups caused the loss of anticancer activity.

Among the six-membered heterocyclic rings (piperidine, morpholine, and piperazine) attached to the 4th position of the benzylidene motif, the piperazine ring gave rise to a significant increase in anticancer activity against A549 cells. On the contrary, the introduction of the pyrrolidine scaffold into the 4th position of the benzylidene group (compound **3h**) resulted in the loss of anticancer activity. Taking into account the IC$_{50}$ values of compounds **3i** and **3j** (Table 1), the 1*H*-imidazole core increased the cytotoxic effect on A549 cell line, while the 1*H*-1,2,4-triazole ring caused the loss of anticancer activity.

Further studies were carried out for compounds **3a**, **3e**, **3g**, and **3i** to illuminate their mechanism of anti-NSCLC action. In this context, after incubation of A549 cells exposed to these agents and cisplatin for 24 h, flow cytometry-based apoptosis detection assay was performed. The percentages of A549 cells undergoing early apoptosis caused by compounds **3a**, **3e**, **3g**, **3i**, and cisplatin (at 91.35, 176.23, 46.60, 83.59, and 23.89 μM, respectively) were found to be 11.22, 3.26, 7.13, 2.70, and 3.61%, respectively (Table 2, Figure 2). The percentages of late apoptotic cells induced by compounds **3a**, **3e**, **3g**, **3i**, and cisplatin were determined as 4.97, 1.76, 12.17, 6.04, and 3.14%, respectively. In particular, compounds **3a** and **3g** showed more apoptotic activity than cisplatin in A549 cells.

A colorimetric method was used to assess the inhibitory effects of compounds **3a**, **3e**, **3g**, and **3i** on Akt in A549 cells. Compound **3e** carrying a piperidine ring in the 4th position of the benzylidene motif and compound **3i** bearing an imidazole ring in the 4th position of the benzylidene moiety inhibited Akt in A549 cells with IC$_{50}$ values of 105.88 ± 53.71 and 69.45 ± 1.48 μM, respectively, compared to GSK690693 (IC$_{50}$ = 5.93 ± 1.20 μM), a well-known Akt inhibitor. According to the data indicated in Table 3, it can be concluded that compounds

https://doi.org/10.1021/acsomega.3c02331
ACS Omega 2023, 8, 20056−20065

Scheme 1. Synthesis of Compounds 3a–j[a]

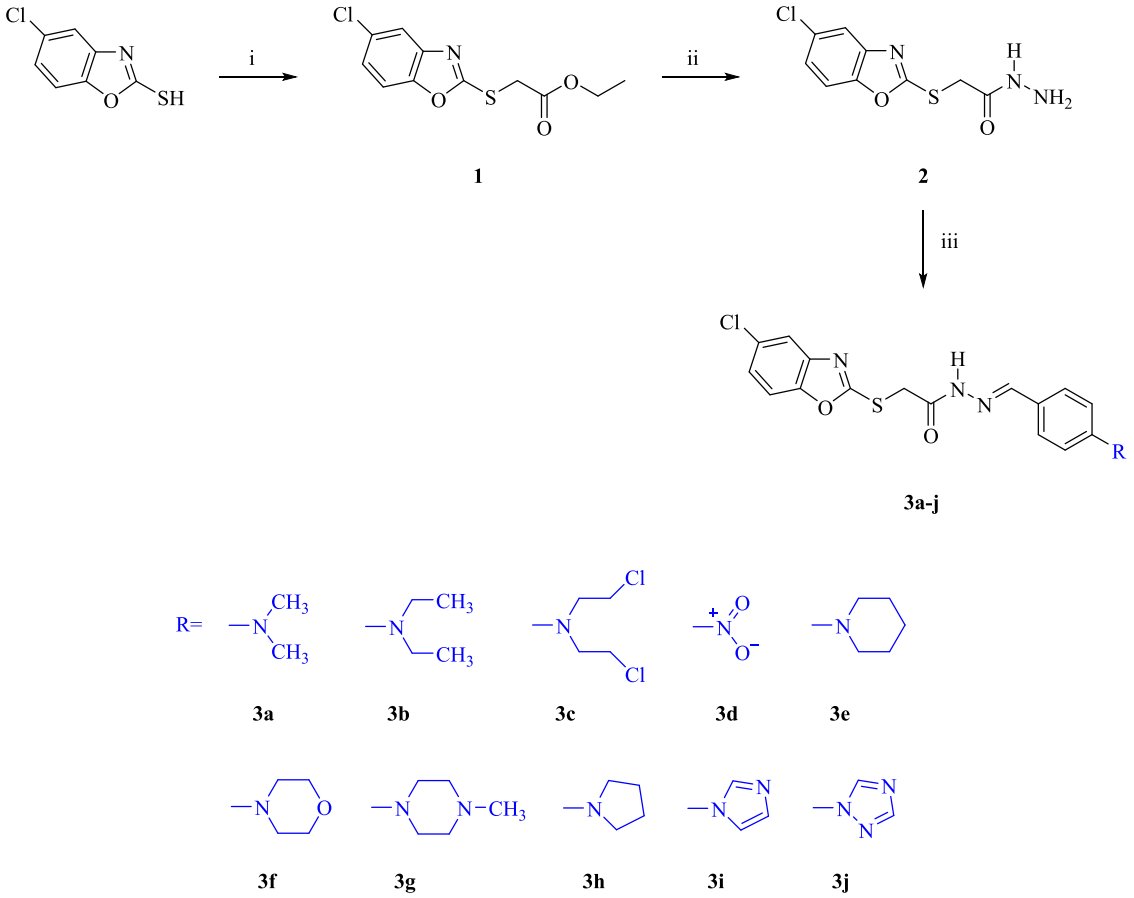

[a](i) $ClCH_2COOEt$, K_2CO_3, acetone, reflux, 10 h; (ii) $NH_2NH_2.H_2O$, ethanol, stirring at room temperature, 5 h; (iii) ArCHO, ethanol, reflux, 8 h.

Table 1. IC_{50} and SI Data for Compounds 2, 3a–j, and Cisplatin

compound	IC_{50} (μM)		SI[a]
	A549 cell line	L929 cell line	
2	>500	>500	
3a	91.35 ± 21.89	>500	>5.47
3b	410.15 ± 220.38	>500	
3c	>500	>500	
3d	>500	>500	
3e	176.23 ± 56.50	>500	>2.84
3f	250.61 ± 45.87	>500	
3g	46.60 ± 6.15	276.67 ± 28.87	5.94
3h	>500	>500	
3i	83.59 ± 7.30	>500	>5.98
3j	>500	>500	
Cisplatin	23.89 ± 2.71		

[a]SI = IC_{50} for L929 cells/IC_{50} for A549 cells.

3e and **3i** exert their anti-NSCLC action through the inhibition of Akt.

Dimethylamino-substituted compound **3a** caused 35.40 ± 13.36% Akt inhibition at 91.35 μM. Compound **3g**, which carries the 4-methylpiperazine motif in the 4th position of the benzylidene moiety, did not exert any inhibitory effect on Akt. Accordingly, it is obvious that both compounds cause cytotoxicity and apoptosis in A549 cell line *via* different pathway(s).

Table 2. Percents of Typical Quadrant Analysis of Annexin V Fluorescein Isothiocyanate (FITC)/PI Flow Cytometry of A549 Cells Exposed to Compounds 3a, 3e, 3g, 3i, and Cisplatin

groups	early apoptosis (%)	late apoptosis (%)	necrosis (%)	viability (%)
control	3.30	1.69	0.24	94.76
cells treated with compound **3a**	11.22	4.97	0.79	83.01
cells treated with compound **3e**	3.26	1.76	3.79	91.19
cells treated with compound **3g**	7.13	12.17	0.78	79.93
cells treated with compound **3i**	2.70	6.04	3.51	87.75
cells treated with **cisplatin**	3.61	3.14	0.98	92.26

2.3. *In Silico* Studies. Computer-aided drug design tools provide a detailed picture of the biologically active molecules at the molecular level. Our recent successful *in silico* studies[40−42] prompted us to confer molecular docking simulations as a tool to enlighten binding conformations of the ligands.

Before moving forward to *in silico* calculations, internal validation[43] was carried out to test how well our docking method performs. The conformation of co-crystallized ligand (GSK690693) was successfully reproduced with Glide XP

https://doi.org/10.1021/acsomega.3c02331
ACS Omega 2023, 8, 20056−20065

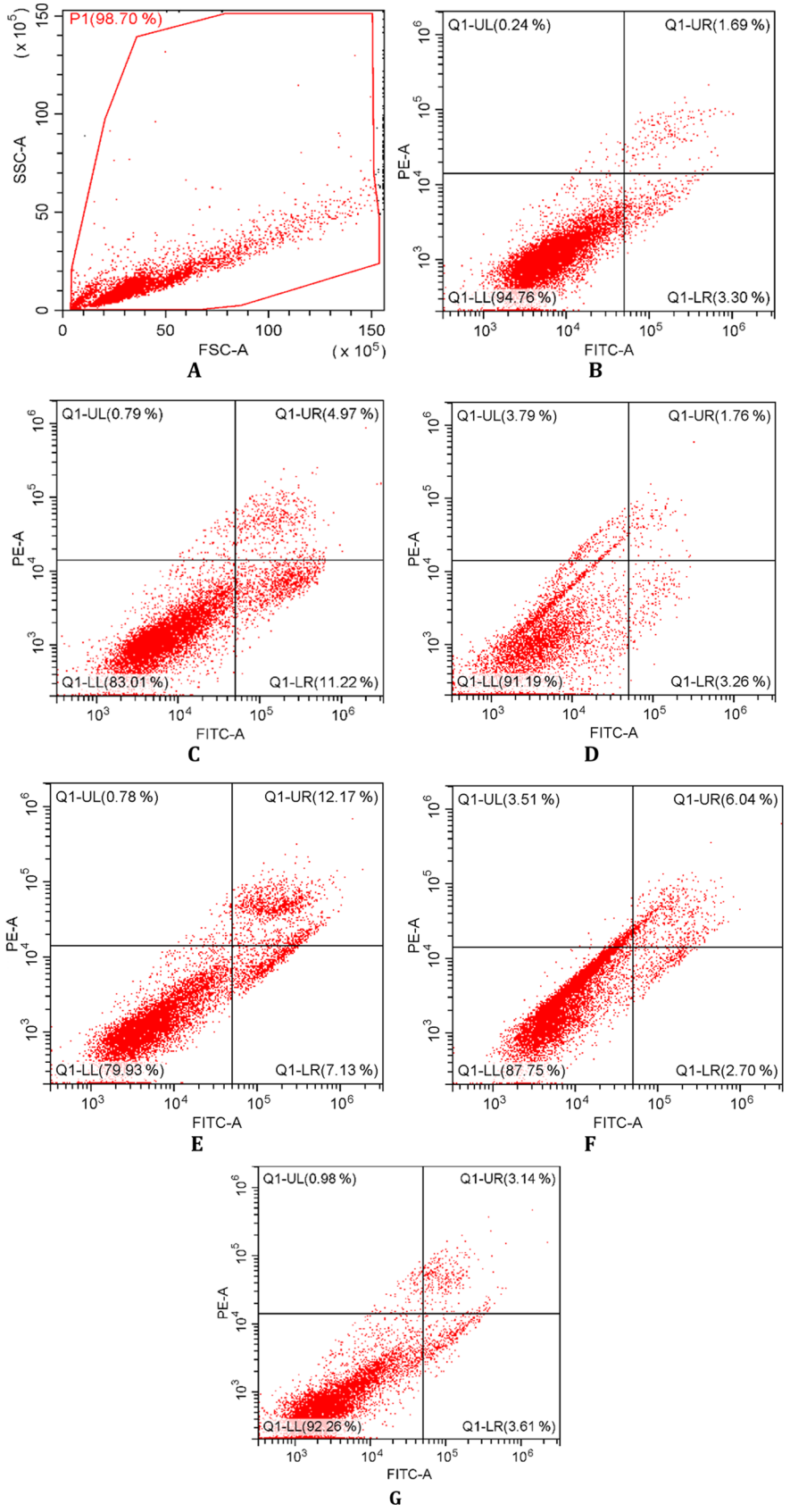

Figure 2. Flow cytometric analysis of A549 cells treated with IC_{50} values of compounds **3a**, **3e**, **3g**, **3i**, and cisplatin. At least 10,000 cells were analyzed per sample, and quadrant analysis was performed. Q1-UL, Q1-LL, Q1-UR, and Q1-LR quadrants represent necrosis, viability, and late and early apoptosis, respectively. (A) The main gate selected from the cell population, (B) control, (C) compound **3a**, (D) compound **3e**, (E) compound **3g**, (F) compound **3i**, and (G) cisplatin.

https://doi.org/10.1021/acsomega.3c02331
ACS Omega 2023, 8, 20056−20065

Table 3. Akt Inhibitory Effects of Compounds 3a, 3e, 3g, 3i, GSK690693, and Cisplatin in A549 Cell Line

compound	IC_{50} (μM)
3a	
3e	105.88 ± 53.71
3g	
3i	69.45 ± 1.48
GSK690693	5.93 ± 1.20
Cisplatin	8.09 ± 0.63

method yielding a root-mean-square deviation (RMSD) of 0.436.

Molecular docking studies showed the binding mode of compound **3i** within Akt2 binding site (Figure 3). The imidazole nitrogen engages in a key hydrogen bond with the backbone amine of ALA232 in the hinge region. The sulfur linker seems to facilitate compound **3i** to adopt a unique binding mode. This folded mode that resembles a V-shaped conformation brings the benzoxazole ring to the vicinity of the acidic pocket. A new hydrogen bond is observed between ASP293 and the N−H of the hydrazide spacer. The interaction of a ligand with this acidic pocket was reported to be important for potent inhibition.[44]

Certain descriptors related to absorption, distribution, metabolism, and excretion (ADME) were also predicted. Blood−brain barrier parameter was also calculated that could be useful in central nervous system-targeted studies. Of note is that compounds **3a**, **3e**, **3g**, and **3i** were estimated to have good pharmacokinetic profiles and druglike properties (Table 4).

3. CONCLUSIONS

This paper describes the synthesis of new hydrazones (**3a**−**j**) designed as small molecules for NSCLC therapy. Taking into account *in vitro* cytotoxicity data, selective anticancer agents in this series on A549 cells were determined as compounds **3a** (IC_{50} = 91.35 ± 21.89 μM), **3e** (IC_{50} = 176.23 ± 56.50 μM), **3g** (IC_{50} = 46.60 ± 6.15 μM), and **3i** (IC_{50} = 83.59 ± 7.30 μM). Among them, compounds **3a** and **3g** caused induction of apoptosis in A549 cells stronger than cisplatin. Both compounds did not exert any significant Akt inhibitory activity in A549 cells, while compounds **3e** and **3i** caused Akt inhibition in A549 cells. It can be concluded that compounds **3e** and **3i** exert their cytotoxic action against A549 cell line *via* the inhibition of Akt. Molecular docking simulations disclosed a unique binding mode for compound **3i** (the most active Akt inhibitor in this series) which interacts with the hinge region and the acidic pocket of Akt2. On the other hand, further research is required to shed light on the mechanism of action underlying the cytotoxic and apoptotic effects of compounds **3a** and **3g** on A549 cells.

4. MATERIALS AND METHODS

4.1. Chemistry. The chemicals were procured from Acros Organics (Geel, Belgium), Maybridge (Loughborough, UK), Merck (Darmstadt, Germany), and Sigma-Aldrich (St. Louis, MO, USA). Melting points (M.p.) were determined by an Electrothermal IA9200 digital melting point apparatus (Staffordshire, U.K.). IR spectra were acquired from an IRPrestige-21 Fourier Transform (FT)-IR spectrophotometer (Shimadzu, Tokyo, Japan). ^{1}H and ^{13}C NMR spectra were recorded on a Varian Mercury-400 FT-NMR spectrometer (Agilent, Palo Alto, CA, USA). HRMS spectra were acquired from an LCMS-IT-TOF (Shimadzu, Kyoto, Japan) using the electrospray ionization (ESI) technique. Thin-layer chromatography (TLC) was employed to track the progress of all chemical reactions and examine the purity of the synthesized agents.

4.1.1. Synthesis of Ethyl 2-[(5-chlorobenzoxazol-2-yl)-thio]acetate (1). A mixture of 5-chloro-2-mercaptobenzoxazole (0.06 mol), potassium carbonate (0.06 mol), and ethyl chloroacetate (0.06 mol) in acetone (60 mL) was heated under reflux for 10 h. The precipitated ester was filtered off and

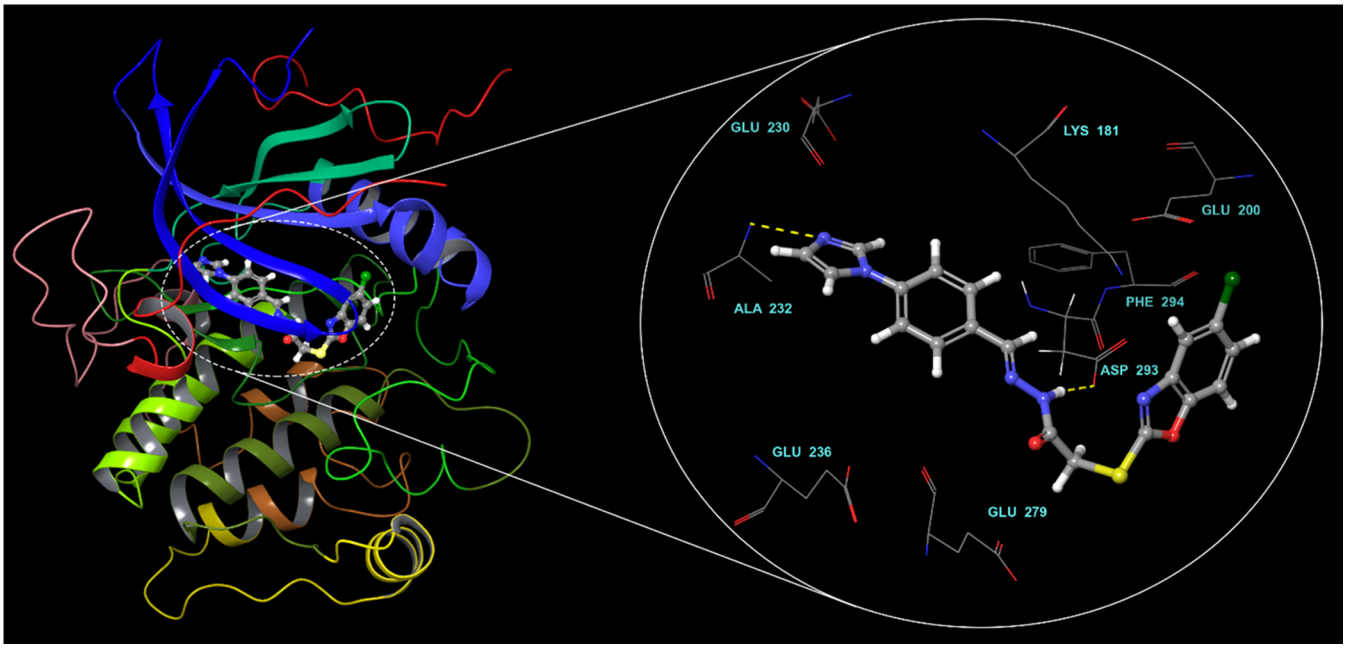

Figure 3. Binding mode of compound **3i** within the binding region of Akt2.

https://doi.org/10.1021/acsomega.3c02331
ACS Omega 2023, 8, 20056−20065

Table 4. Predicted ADME Properties of Compounds 3a, 3e, 3g, and 3i[a]

compound	MW	QPlogPo/w	QPlogBB[b]	HOA%[c]	PSA[d]	rule of five[e]
3a	388.87	4.65	−0.77	100.00	76.85	0.00
3e	428.94	5.41	−0.79	100.00	78.08	1.00
3g	443.95	4.09	−0.26	94.58	82.42	0.00
3i	411.87	4.54	−1.06	100.00	89.18	0.00

[a]Octanol/water partition coefficient (recommended range: −2.0 to 6.5). [b]Brain/blood partition coefficient (recommended range: −3.0 to 1.2). [c]Human oral absorption (HOA) (<25% is poor, >80% is high). [d]Polar surface area (PSA) (recommended range: 7.0−200.0). [e]Number of violations of Lipinski's rule of five.

washed with distilled water. After drying, the product was crystallized from ethanol.

Yield: 98%, M.p.: 65−67 °C, Lit. M.p.: 64−65 °C.[45] IR ν_{max} (cm^{-1}): 3091.89, 3068.75, 3022.45, 2978.09, 2931.80, 1735.93, 1612.49, 1496.76, 1462.04, 1446.61, 1429.25, 1375.25, 1309.67, 1257.59, 1234.44, 1219.01, 1193.94, 1174.65, 1141.86, 1109.07, 1058.92, 1026.13, 937.40, 920.05, 898.83, 867.97, 860.25, 819.75, 767.67, 715.59, 702.09, 677.01. ^{1}H NMR (400 MHz, DMSO-d_6) δ (ppm): 1.19 (t, J = 7.0 Hz, 3H), 4.16 (q, J = 7.2 Hz, 2H), 4.30 (s, 2H), 7.36 (dd, J = 8.4 Hz, 2.0 Hz, 1H), 7.68 (d, J = 9.2 Hz, 1H), 7.74 (d, J = 2.4 Hz, 1H). ^{13}C NMR (100 MHz, DMSO-d_6) δ (ppm): 13.97 (CH_3), 33.78 (CH_2), 61.57 (CH_2), 111.54 (CH), 118.12 (CH), 124.34 (CH), 129.01 (C), 142.37 (C), 150.15 (C), 165.45 (C), 167.69 (C). HRMS (ESI) (m/z): $[M + H]^+$ calcd for $C_{11}H_{10}ClNO_3S$: 272.0143, found, 272.0141.

*4.1.2. Synthesis of 2-[(5-Chlorobenzoxazol-2-yl)thio]-acetohydrazide (**2**).* A mixture of compound **1** (0.05 mol) and hydrazine hydrate (0.10 mol) was stirred in ethanol for 5 h at room temperature. The precipitated hydrazide was filtered off and washed with ethanol. After drying, it was crystallized from ethanol.

Yield: 66%, M.p.: 159−161 °C, Lit. M.p.: 190−192 °C.[45] IR ν_{max} (cm^{-1}): 3284.77, 3157.47, 3068.75, 2999.31, 2953.02, 2873.94, 1651.07, 1629.85, 1548.84, 1494.83, 1465.90, 1448.54, 1423.47, 1406.11, 1338.60, 1253.73, 1238.30, 1211.30, 1136.07, 1105.21, 1051.20, 1010.70, 956.69, 933.55, 918.12, 864.11, 821.68, 806.25, 773.46, 729.09, 686.66. ^{1}H NMR (400 MHz, DMSO-d_6) δ (ppm): 3.35 (brs, 1H), 4.10 (s, 2H), 4.40 (brs, 1H), 7.35 (dd, J = 8.6 Hz, 2.2 Hz, 1H), 7.67 (d, J = 8.8 Hz, 1H), 7.72 (d, J = 2.4 Hz, 1H), 8.86 and 9.44 (2brs, 1H). ^{13}C NMR (100 MHz, DMSO-d_6) δ (ppm): 34.06 (CH_2), 111.50 (CH), 117.99 (CH), 124.24 (CH), 128.93 (C), 142.50 (C), 150.09 (C), 165.45 (C), 165.87 (C). HRMS (ESI) (m/z): $[M + H]^+$ calcd for $C_9H_8ClN_3O_2S$: 258.0099, found, 258.0109.

*4.1.3. General Procedure for the Preparation of N′-(4-Subsittuted benzylidene)-2-[(5-chlorobenzoxazol-2-yl)thio]-acetohydrazide (**3a−j**).* A mixture of compound **2** (0.0012 mol) and 4-substituted benzaldehyde (0.0012 mol) was heated under reflux in ethanol for 8 h. The precipitate was filtered off and washed with ethanol. After drying, the product was crystallized from ethanol.

*4.1.3.1. N′-(4-Dimethylaminobenzylidene)-2-[(5-chloro-benzoxazol-2-yl)thio]acetohydrazide (**3a**).* Yield: 62%, M.p.: 197−199 °C. IR ν_{max} (cm^{-1}): 3167.12, 3074.53, 3018.60, 2951.09, 2889.37, 1666.50, 1602.85, 1535.34, 1492.90, 1456.26, 1442.75, 1402.25, 1365.60, 1317.38, 1249.87, 1230.58, 1209.37, 1178.51, 1159.22, 1134.14, 1101.35, 1051.20, 948.98, 937.40, 918.12, 854.47, 819.75, 808.17, 796.60, 786.96, 702.09, 669.30. ^{1}H NMR (400 MHz, DMSO-d_6) δ (ppm): 2.96 (s, 6H), 4.25 and 4.65 (2s, 2H), 6.71 (d, J = 8.8 Hz, 2H), 7.35 (d, J = 8.8 Hz, 2.0 Hz, 1H), 7.50 (d, J = 8.8 Hz, 2H), 7.68 (dd, J = 8.8 Hz, 2.6 Hz, 1H), 7.75 (dd, J = 8.4 Hz, 2.0 Hz, 1H), 7.91 and 8.06 (2s, 1H), 11.52 and 11.56 (2brs, 1H). ^{13}C NMR (100 MHz, DMSO-d_6) δ (ppm): 35.02 (CH_2), 39.64 ($2CH_3$), 111.42 (CH), 111.73 (2CH), 118.06 (CH), 121.15 (CH), 124.15 (C), 128.24 (2CH), 128.52 (C), 142.58 (C), 144.96 (CH), 150.10 (C), 151.43 (C), 166.32 (C), 167.19 (C). HRMS (ESI) (m/z): $[M + H]^+$ calcd for $C_{18}H_{17}ClN_4O_2S$: 389.0834, found, 389.0853.

*4.1.3.2. N′-(4-Diethylaminobenzylidene)-2-[(5-chloroben-zoxazol-2-yl)thio]acetohydrazide (**3b**).* Yield: 65%, M.p.: 172−173 °C. IR ν_{max} (cm^{-1}): 3172.90, 3082.25, 2968.45, 2927.94, 2893.22, 1666.50, 1610.56, 1597.06, 1527.62, 1494.83, 1463.97, 1444.68, 1421.54, 1400.32, 1386.82, 1375.25, 1350.17, 1313.52, 1273.02, 1253.73, 1213.23, 1197.79, 1182.36, 1155.36, 1134.14, 1105.21, 1082.07, 1051.20, 1012.63, 1004.91, 954.76, 929.69, 914.26, 881.47, 860.25, 813.96, 779.24, 758.02, 715.59, 700.16, 677.01. ^{1}H NMR (400 MHz, DMSO-d_6) δ (ppm): 1.09 (t, J = 7.0 Hz, 6H), 3.34−3.39 (m, 4H), 4.25 and 4.64 (2s, 2H), 6.65 (d, J = 8.8 Hz, 2H), 7.35 (dd, J = 8.6 Hz, 2.2 Hz, 1H), 7.45 (d, J = 8.8 Hz, 2H), 7.69 (dd, J = 8.6 Hz, 1.8 Hz, 1H), 7.75 (dd, J = 10.0 Hz, 2.0 Hz, 1H), 7.88 and 8.03 (2s, 1H), 11.49 and 11.52 (2s, 1H). ^{13}C NMR (100 MHz, DMSO-d_6) δ (ppm): 12.41 ($2CH_3$), 35.01 (CH_2), 43.74 ($2CH_2$), 111.02 (2CH), 111.47 (CH), 118.06 (CH), 120.22 (CH), 124.15 (C), 128.57 (2CH), 128.91 (C), 142.59 (C), 145.00 (CH), 148.77 (C), 150.11 (C), 166.33 (C), 167.14 (C). HRMS (ESI) (m/z): $[M + H]^+$ calcd for $C_{20}H_{21}ClN_4O_2S$: 417.1147, found, 417.1171.

*4.1.3.3. N′-[4-(Bis(2-chloroethyl)amino)benzylidene]-2-[(5-chlorobenzoxazol-2-yl)thio]acetohydrazide (**3c**).* Yield: 47%, M.p.: 155−156 °C. IR ν_{max} (cm^{-1}): 3180.62, 3072.60, 3012.81, 2962.66, 2895.15, 1662.64, 1598.99, 1525.69, 1510.26, 1494.83, 1448.54, 1413.82, 1390.68, 1355.96, 1315.45, 1276.88, 1255.66, 1203.58, 1176.58, 1136.07, 1107.14, 1053.13, 958.62, 929.69, 916.19, 910.40, 864.11, 815.89, 804.32, 746.45, 717.52, 678.94. ^{1}H NMR (400 MHz, DMSO-d_6) δ (ppm): 3.74−3.79 (m, 8H), 4.26 and 4.65 (2s, 2H), 6.79 (d, J = 9.2 Hz, 2H), 7.35 (dd, J = 8.4 Hz, 2.4 Hz, 1H), 7.52 (d, J = 9.2 Hz, 2H), 7.68 (dd, J = 8.6 Hz, 2.2 Hz, 1H), 7.74 (dd, J = 9.0 Hz, 2.2 Hz, 1H), 7.91 and 8.07 (2s, 1H), 11.56 and 11.60 (2s, 1H). ^{13}C NMR (100 MHz, DMSO-d_6) δ (ppm): 35.00 (CH_2), 40.98 ($2CH_2$), 51.85 ($2CH_2$), 111.46 (CH), 111.76 (2CH), 118.06 (CH), 122.29 (CH), 124.15 (C), 128.59 (2CH), 128.91 (C), 142.56 (C), 144.53 (CH), 147.94 (C), 150.11 (C), 166.28 (C), 167.31 (C). HRMS (ESI) (m/z): $[M + H]^+$ calcd for $C_{20}H_{19}Cl_3N_4O_2S$: 485.0367, found, 485.0394.

*4.1.3.4. N′-(4-Nitrobenzylidene)-2-[(5-chlorobenzoxazol-2-yl)thio]acetohydrazide (**3d**).* Yield: 88%, M.p.: 237−239 °C. IR ν_{max} (cm^{-1}): 3201.83, 3093.82, 2960.73, 2846.93, 1680.00, 1614.42, 1597.06, 1585.49, 1516.05, 1487.12,

https://doi.org/10.1021/acsomega.3c02331
ACS Omega 2023, 8, 20056−20065

1452.40, 1404.18, 1379.10, 1336.67, 1255.66, 1226.73, 1201.65, 1151.50, 1139.93, 1112.93, 1105.21, 1064.71, 929.69, 918.12, 898.83, 889.18, 860.25, 850.61, 833.25, 821.68, 804.32, 748.38, 736.81, 704.02, 690.52. ^{1}H NMR (400 MHz, DMSO-d_6) δ (ppm): 4.33 and 4.73 (2s, 2H), 7.35 (dd, J = 8.6 Hz, 1.8 Hz, 1H), 7.68 (dd, J = 8.8 Hz, 4.8 Hz, 1H), 7.73−7.74 (m, 1H), 7.96−7.99 (m, 2H), 8.14 (s, 1H), 8.26−8.32 (m, 2H), 12.09 (brs, 1H). ^{13}C NMR (100 MHz, DMSO-d_6) δ (ppm): 34.76 (CH_2), 111.48 (CH), 118.06 (CH), 124.02 (2CH), 124.21 (CH), 127.89 (2CH), 128.94 (C), 140.14 (C), 142.49 (C), 144.87 (CH), 147.80 (C), 150.11 (C), 166.02 (C), 168.27 (C). HRMS (ESI) (m/z): [M + H]$^+$ calcd for $C_{16}H_{11}ClN_4O_4S$: 391.0262, found, 391.0278.

*4.1.3.5. N′-[4-(Piperidin-1-yl)benzylidene]-2-[(5-chlorobenzoxazol-2-yl)thio]acetohydrazide (**3e**).* Yield: 77%, M.p.: 187−188 °C. IR ν_{max} (cm^{-1}): 3165.19, 3076.46, 3008.95, 2920.23, 2850.79, 1664.57, 1600.92, 1523.76, 1494.83, 1456.26, 1442.75, 1425.40, 1386.82, 1354.03, 1315.45, 1226.73, 1209.37, 1184.29, 1163.08, 1126.43, 1099.43, 1051.20, 1020.34, 952.84, 935.48, 918.12, 852.54, 806.25, 794.67, 715.59, 702.09, 677.01. ^{1}H NMR (400 MHz, DMSO-d_6) δ (ppm): 1.56 (brs, 6H), 3.24 (brs, 4H), 4.26 and 4.65 (2s, 2H), 6.91−6.95 (m, 2H), 7.35 (dd, J = 8.8 Hz, 2.0 Hz, 1H), 7.50 (dd, J = 8.6 Hz, 5.0 Hz, 2H), 7.68 (dd, J = 8.6 Hz, 3.0 Hz, 1H), 7.74 (dd, J = 7.8 Hz, 1.8 Hz, 1H), 7.91 and 8.06 (2s, 1H), 11.56 and 11.61 (2s, 1H). ^{13}C NMR (100 MHz, DMSO-d_6) δ (ppm): 23.92 (CH_2), 24.95 ($2CH_2$), 34.98 (CH_2), 48.40 ($2CH_2$), 111.47 (CH), 114.58 (2CH), 118.06 (CH), 122.94 (CH), 124.15 (C), 128.18 (2CH), 128.47 (C), 142.57 (C), 144.62 (CH), 150.11 (C), 152.35 (C), 166.28 (C), 167.30 (C). HRMS (ESI) (m/z): [M + H]$^+$ calcd for $C_{21}H_{21}ClN_4O_2S$: 429.1147, found, 429.1153.

*4.1.3.6. N′-[4-(Morpholin-4-yl)benzylidene]-2-[(5-chlorobenzoxazol-2-yl)thio]acetohydrazide (**3f**).* Yield: 82%, M.p.: 209−210 °C. IR ν_{max} (cm^{-1}): 3180.62, 3078.39, 3010.88, 2962.66, 2854.65, 1666.50, 1604.77, 1523.76, 1498.69, 1446.61, 1425.40, 1400.32, 1381.03, 1311.59, 1269.16, 1253.73, 1228.66, 1211.30, 1184.29, 1166.93, 1132.21, 1122.57, 1111.00, 1101.35, 1051.20, 948.98, 927.76, 918.12, 862.18, 819.75, 808.17, 792.74, 717.52, 702.09, 677.01. ^{1}H NMR (400 MHz, DMSO-d_6) δ (ppm): 3.19 (t, J = 4.8 Hz, 2H), 3.28 (t, J = 4.8 Hz, 2H), 3.71−3.75 (m, 4H), 4.26 and 4.66 (2s, 2H), 6.87 (d, J = 8.8 Hz, 2H), 7.35 (dd, J = 8.6 Hz, 2.2 Hz, 1H), 7.55 (d, J = 8.8 Hz, 2H), 7.69 (dd, J = 8.6 Hz, 3.8 Hz, 1H), 7.73 (d, J = 8.8 Hz, 1H), 7.94 and 8.10 (2s, 1H), 11.63 (brs, 1H). ^{13}C NMR (100 MHz, DMSO-d_6) δ (ppm): 34.91 (CH_2), 46.90 ($2CH_2$), 65.82 ($2CH_2$), 111.44 (CH), 113.78 (2CH), 117.51 (CH), 122.25 (CH), 124.55 (C), 128.09 (C), 130.12 (2CH), 142.55 (C), 144.46 (CH), 150.09 (C), 152.16 (C), 166.24 (C), 167.37 (C). HRMS (ESI) (m/z): [M + H]$^+$ calcd for $C_{20}H_{19}ClN_4O_3S$: 431.0939, found, 431.0954.

*4.1.3.7. N′-[4-(4-Methylpiperazin-1-yl)benzylidene]-2-[(5-chlorobenzoxazol-2-yl)thio]acetohydrazide (**3g**).* Yield: 35%, M.p.: 178−179 °C. IR ν_{max} (cm^{-1}): 3205.69, 3061.03, 2949.16, 2935.66, 2845.00, 2802.57, 1654.92, 1610.56, 1600.92, 1562.34, 1517.98, 1496.76, 1448.54, 1425.40, 1409.96, 1381.03, 1361.74, 1315.45, 1294.24, 1251.80, 1234.44, 1209.37, 1190.08, 1161.15, 1130.29, 1107.14, 1078.21, 1055.06, 999.13, 960.55, 918.12, 875.68, 819.75, 794.67, 700.16, 673.16. ^{1}H NMR (400 MHz, DMSO-d_6) δ (ppm): 2.23 (s, 3H), 2.45 (t, J = 4.8 Hz, 4H), 3.24 (t, J = 4.6 Hz, 4H), 4.28 and 4.67 (2s, 2H), 6.96−6.99 (m, 2H), 7.37 (dd, J = 8.6 Hz, 1.8 Hz, 1H), 7.55 (dd, J = 9.2 Hz, 4.4 Hz, 2H), 7.70 (dd, J = 8.6 Hz, 3.4 Hz, 1H), 7.76 (dd, J = 7.4 Hz, 1.8 Hz, 1H), 7.94 and 8.10 (2s, 1H), 11.60 and 11.66 (2s, 1H). ^{13}C NMR (100 MHz, DMSO-d_6) δ (ppm): 34.97 (CH_2), 45.74 (CH_3), 47.09 ($2CH_2$), 54.40 ($2CH_2$), 111.47 (CH), 114.50 (2CH), 118.07 (CH), 123.63 (CH), 124.17 (C), 128.16 (2CH), 128.40 (C), 128.91 (C), 142.57 (C), 144.53 (CH), 150.11 (C), 166.28 (C), 167.35 (C). HRMS (ESI) (m/z): [M + H]$^+$ calcd for $C_{21}H_{22}ClN_5O_2S$: 444.1255, found, 444.1278.

*4.1.3.8. N′-[4-(Pyrrolidin-1-yl)benzylidene]-2-[(5-chlorobenzoxazol-2-yl)thio]acetohydrazide (**3h**).* Yield: 82%, M.p.: 206−207 °C. IR ν_{max} (cm^{-1}): 3170.97, 3080.32, 2976.16, 2956.87, 2096.73, 2850.79, 1666.50, 1612.49, 1598.99, 1529.55, 1494.83, 1448.54, 1436.97, 1386.82, 1348.24, 1315.45, 1301.95, 1249.87, 1217.08, 1178.51, 1163.08, 1138.00, 1107.14, 1049.28, 958.62, 931.62, 916.19, 902.69, 858.32, 810.10, 779.24, 700.16, 675.09. ^{1}H NMR (400 MHz, DMSO-d_6) δ (ppm): 1.93−1.98 (m, 4H), 3.26 (t, J = 6.6 Hz, 4H), 4.25 and 4.64 (2s, 2H), 6.52−6.56 (m, 2H), 7.35 (dd, J = 8.6 Hz, 2.2 Hz, 1H), 7.48 (dd, J = 9.0 Hz, 5.0 Hz, 2H), 7.66−7.69 (m, 1H), 7.74 (dd, J = 8.4 Hz, 2.0 Hz, 1H), 7.89 and 8.05 (2s, 1H), 11.47 and 11.51 (2s, 1H). ^{13}C NMR (100 MHz, DMSO-d_6) δ (ppm): 24.93 ($2CH_2$), 34.99 (CH_2), 47.19 ($2CH_2$), 111.42 (CH), 111.49 (2CH), 118.03 (CH), 122.25 (CH), 124.12 (C), 128.36 (2CH), 128.64 (C), 142.57 (C), 145.19 (CH), 148.82 (C), 150.08 (C), 166.30 (C), 167.08 (C). HRMS (ESI) (m/z): [M + H]$^+$ calcd for $C_{20}H_{19}ClN_4O_2S$: 415.0990, found, 415.1013.

*4.1.3.9. N′-[4-(1H-Imidazol-1-yl)benzylidene]-2-[(5-chlorobenzoxazol-2-yl)thio]acetohydrazide (**3i**).* Yield: 83%, M.p.: 229−231 °C. IR ν_{max} (cm^{-1}): 3159.40, 3099.61, 2978.09, 2823.79, 1705.07, 1608.63, 1577.77, 1521.84, 1487.12, 1465.90, 1448.54, 1427.32, 1400.32, 1359.82, 1305.81, 1263.37, 1228.66, 1215.15, 1176.58, 1136.07, 1107.14, 1060.85, 989.48, 962.48, 927.76, 916.19, 866.04, 835.18, 817.82, 719.45, 702.09, 680.87, 651.94. ^{1}H NMR (400 MHz, DMSO-d_6) δ (ppm): 4.31 and 4.71 (2s, 2H), 7.14 (brs, 1H), 7.34 (dd, J = 8.4 Hz, 2.4 Hz, 1H), 7.68 (dd, J = 8.6 Hz, 5.0 Hz, 1H), 7.73−7.76 (m, 3H), 7.82−7.86 (m, 3H), 8.08 and 8.26 (2s, 1H), 8.35 (brs, 1H), 11.86 and 11.92 (2s, 1H). ^{13}C NMR (100 MHz, DMSO-d_6) δ (ppm): 34.81 (CH_2), 111.44 (CH), 117.78 (CH), 118.03 (CH), 120.29 (2CH), 124.17 (CH), 128.38 (2CH), 128.90 (CH), 130.13 (C), 132.28 (C), 135.54 (CH), 137.80 (C), 142.51 (C), 143.05 (CH), 150.09 (C), 166.11 (C), 167.89 (C). HRMS (ESI) (m/z): [M + H]$^+$ calcd for $C_{19}H_{14}ClN_5O_2S$: 412.0629, found, 412.0659.

*4.1.3.10. N′-[4-(1H-1,2,4-Triazol-1-yl)benzylidene]-2-[(5-chlorobenzoxazol-2-yl)thio]acetohydrazide (**3j**).* Yield: 80%, M.p.: 256−257 °C. IR ν_{max} (cm^{-1}): 3207.62, 3124.68, 3088.03, 2951.09, 2829.57, 1670.35, 1614.42, 1523.76, 1492.90, 1452.40, 1402.25, 1373.32, 1344.38, 1319.31, 1280.73, 1246.02, 1219.01, 1201.65, 1143.79, 1107.14, 1051.20, 979.84, 960.55, 916.19, 889.18, 833.25, 819.75, 790.81, 702.09, 671.23. ^{1}H NMR (400 MHz, DMSO-d_6) δ (ppm): 4.29 and 4.72 (2s, 2H), 7.34 (dd, J = 8.6 Hz, 2.2 Hz, 1H), 7.67 (dd, J = 8.6 Hz, 5.0 Hz, 1H), 7.72−7.74 (m, 1H), 7.87−7.96 (m, 4H), 8.09 and 8.26 (2s, 1H), 8.27 (s, 1H), 9.37 (s, 1H), 11.87 (brs, 1H). ^{13}C NMR (100 MHz, DMSO-d_6) δ (ppm): 34.83 (CH_2), 111.43 (CH), 118.03 (CH), 119.49 (2CH), 124.16 (CH), 128.30 (2CH), 128.51 (C), 133.19 (C), 137.51 (C), 142.45 (CH), 142.51 (C), 142.95 (CH), 150.09 (C), 152.57 (CH), 166.10 (C), 167.91 (C). HRMS (ESI) (m/z):

https://doi.org/10.1021/acsomega.3c02331
ACS Omega 2023, 8, 20056−20065

$[M + H]^+$ calcd for $C_{18}H_{13}ClN_6O_2S$: 413.0582, found, 413.0607.

4.2. Biochemistry. *4.2.1. Cell Culture and Drug Treatment.* A549 and L929 cell lines were purchased from American Type Culture Collection (Manassas, VA, USA). Cells were cultured, and drug treatments were performed as previously explained.[46]

4.2.2. MTT Test. MTT assay was conducted as previously described[47] with slight modifications.[48] Cisplatin was used as a positive control. The assay was performed in triplicate. Half-maximal inhibitory concentration (IC_{50}) data (μM) were expressed as mean ± SD.

4.2.3. Flow Cytometric Analyses of Apoptosis. FITC Annexin V Apoptosis Detection Kit (BD Pharmingen, San Jose, CA, USA) was applied using a CytoFLEX flow cytometer (Beckman Coulter, Indianapolis, USA) in accordance with the manufacturer's instructions following the 24 h incubation of A549 cells with compounds **3a**, **3e**, **3g**, **3i**, and cisplatin at 91.35, 176.23, 46.60, 83.59, and 23.89 μM, respectively.

4.2.4. Determination of Akt Inhibition. Akt Colorimetric In-Cell ELISA Kit (Thermo Fisher Scientific, Waltham, MA, USA) was used in accordance with the instructions provided by the manufacturer after A549 cells were incubated with compounds **3a** (22.84, 45.68, and 91.35 μM), **3e** (44.06, 88.12, and 176.23 μM), **3g** (11.65, 23.30, and 46.60 μM), **3i** (20.90, 41.80, and 83.59 μM), cisplatin (5.97, 11.95, and 23.89 μM), and GSK690693 (3.61, 7.23, and 14.45 μM) for 24 h. The assay was performed in triplicate. IC_{50} data (μM) were expressed as mean ± SD.

4.2.5. Statistical Analyses. Statistical Package for the Social Sciences (SPSS) for Windows 15.0 was used for statistical analysis. Comparisons were performed by one-way ANOVA test for normally distributed continuous variables, and post hoc analyses of group differences were expressed by the Tukey test.

4.3. *In Silico* Studies. The crystal structure of human Akt2 in complex with GSK690693 was downloaded from Protein Data Bank (PDB ID: 3D0E at 2.00 Å resolution). This raw protein structure was initially prepared[49] by adding missing hydrogens, correcting bond orders, and removing all heteroatoms except the native ligand. The structure was then optimized to address any overlapping hydrogens, and finally, restrained minimization was carried out.

The binding site of Akt2 was defined by computing grid file using GSK690693 as a reference agent. The size of enclosing box that represents grid was extended to allow docking of the ligands with length <20 Å. Glide XP module[50] was selected for molecular docking. LigPrep module[51] was used to prepare ligands for *in silico* calculations to consider all possible geometries, tautomers, and also protonation states at physiological conditions. Important molecular descriptors related to ADME were predicted using QikProp module.[52]

■ ASSOCIATED CONTENT

Supporting Information

The Supporting Information is available free of charge at https://pubs.acs.org/doi/10.1021/acsomega.3c02331.

IR, ^1H NMR, ^{13}C NMR, and HRMS spectra of compounds **1**, **2**, and **3a**−**j** (PDF)

■ AUTHOR INFORMATION

Corresponding Author

Mehlika Dilek Altıntop − *Department of Pharmaceutical Chemistry, Faculty of Pharmacy, Anadolu University, 26470 Eskişehir, Turkey;* orcid.org/0000-0002-8159-663X; Email: mdaltintop@anadolu.edu.tr

Authors

Burak Erdönmez − *Department of Pharmaceutical Chemistry, Graduate School of Health Sciences, Anadolu University, 26470 Eskişehir, Turkey*

Gülşen Akalın Çiftçi − *Department of Biochemistry, Faculty of Pharmacy, Anadolu University, 26470 Eskişehir, Turkey*

Ahmet Özdemir − *Department of Pharmaceutical Chemistry, Faculty of Pharmacy, Anadolu University, 26470 Eskişehir, Turkey*

Abdulilah Ece − *Department of Pharmaceutical Chemistry, Faculty of Pharmacy, Biruni University, 34010 Istanbul, Turkey;* orcid.org/0000-0002-3087-5145

Complete contact information is available at: https://pubs.acs.org/10.1021/acsomega.3c02331

Author Contributions

M.D.A. and A.Ö. designed the research; B.E. and M.D.A. performed the synthesis and characterization of all compounds; A.E. carried out molecular docking and *in silico* ADME studies; G.A.Ç. performed *in vitro* experimental studies. M.D.A. mainly wrote manuscript. M.D.A. was responsible for the correspondence of the manuscript. All authors discussed, edited, and approved the final version.

Notes

The authors declare no competing financial interest.

■ REFERENCES

(1) Arya, S. K.; Bhansali, S. Lung cancer and its early detection using biomarker based biosensors. *Chem. Rev.* **2011**, *111*, 6783−6809.

(2) Sung, H.; Ferlay, J.; Siegel, R. L.; Laversanne, M.; Soerjomataram, I.; Jemal, A.; Bray, F. Global cancer statistics 2020: GLOBOCAN estimates of incidence and mortality worldwide for 36 cancers in 185 countries. *CA Cancer J. Clin.* **2021**, *71*, 209−249.

(3) Zhu, T.; Bao, X.; Chen, M.; Lin, R.; Zhuyan, J.; Zhen, T.; Xing, K.; Zhou, W.; Zhu, S. Mechanisms and future of non-small cell lung cancer metastasis. *Front. Oncol.* **2020**, *10*, No. 585284.

(4) Janku, F.; Stewart, D. J.; Kurzrock, R. Targeted therapy in non-small-cell lung cancer-is it becoming a reality? *Nat. Rev. Clin. Oncol.* **2010**, *7*, 401−414.

(5) Jayan, A. P.; Anandu, K. R.; Madhu, K.; Saiprabha, V. N. A pharmacological exploration of targeted drug therapy in non-small cell lung cancer. *Med. Oncol.* **2022**, *39*, 147.

(6) Nascimento, A. V.; Bousbaa, H.; Ferreira, D.; Sarmento, B. Non-small cell lung carcinoma: An overview on targeted therapy. *Curr. Drug Targets* **2015**, *16*, 1448−1463.

(7) Li, L.; Zhu, T.; Gao, Y.-F.; Zheng, W.; Wang, C.-J.; Xiao, L.; Huang, M.-S.; Yin, J.-Y.; Zhou, H.-H.; Liu, Z.-Q. Targeting DNA damage response in the radio(chemo)therapy of non-small cell lung cancer. *Int. J. Mol. Sci.* **2016**, *17*, 839.

(8) Iksen; Pothongsrisit, S.; Pongrakhananon, V. Targeting the PI3K/AKT/mTOR signaling pathway in lung cancer: An update regarding potential drugs and natural products. *Molecules* **2021**, *26*, 4100.

(9) Sosa Iglesias, V.; Giuranno, L.; Dubois, L. J.; Theys, J.; Vooijs, M. Drug resistance in non-small cell lung cancer: A potential for NOTCH targeting? *Front. Oncol.* **2018**, *8*, 267.

(10) Chen, K.; Shang, Z.; Dai, A.-l.; Dai, P.-l. Novel PI3K/Akt/mTOR pathway inhibitors plus radiotherapy: Strategy for non-small

cell lung cancer with mutant RAS gene. *Life Sci.* **2020**, *255*, No. 117816.
(11) Huang, J.; Chen, L.; Wu, J.; Ai, D.; Zhang, J. Q.; Chen, T. G.; Wang, L. Targeting the PI3K/AKT/mTOR signaling pathway in the treatment of human diseases: Current status, trends, and solutions. *J. Med. Chem.* **2022**, *65*, 16033−16061.
(12) Song, M.; Bode, A. M.; Dong, Z.; Lee, M. H. AKT as a therapeutic target for cancer. *Cancer Res.* **2019**, *79*, 1019−1031.
(13) Nitulescu, G. M.; Margina, D.; Juzenas, P.; Peng, Q.; Olaru, O. T.; Saloustros, E.; Fenga, C.; Spandidos, D. A.; Libra, M.; Tsatsakis, A. M. Akt inhibitors in cancer treatment: The long journey from drug discovery to clinical use (Review). *Int. J. Oncol.* **2016**, *48*, 869−885.
(14) Mali, S. N.; Thorat, B. R.; Gupta, D. R.; Pandey, A. Mini-review of the importance of hydrazides and their derivatives-Synthesis and biological activity. *Eng. Proc.* **2021**, *11*, 21.
(15) Popiołek, Ł. Hydrazide-hydrazones as potential antimicrobial agents: Overview of the literature since 2010. *Med. Chem. Res.* **2017**, *26*, 287−301.
(16) Mathew, B.; Suresh, J.; Ahsan, M. J.; Mathew, G. E.; Usman, D.; Subramanyan, P. N. S.; Safna, K. F.; Maddela, S. Hydrazones as a privileged structural linker in antitubercular agents: A review. *Infect. Disord. Drug Targets* **2015**, *15*, 76−88.
(17) Wahbeh, J.; Milkowski, S. The use of hydrazones for biomedical applications. *SLAS Technol.* **2019**, *24*, 161−168.
(18) Rollas, S.; Küçükgüzel, S. G. Biological activities of hydrazone derivatives. *Molecules* **2007**, *12*, 1910−1939.
(19) Altıntop, M. D.; Akalın Çiftçi, G.; Yılmaz Savaş, N.; Ertorun, İ.; Can, B.; Sever, B.; Temel, H. E.; Alataş, Ö.; Özdemir, A. Discovery of small molecule COX-1 and Akt inhibitors as anti-NSCLC agents endowed with anti-inflammatory action. *Int. J. Mol. Sci.* **2023**, *24*, 2648.
(20) Şenkardeş, S.; Han, M.İ.; Gürboğa, M.; Bingöl Özakpinar, Ö.; Küçükgüzel, Ş.G. Synthesis and anticancer activity of novel hydrazone linkage-based aryl sulfonate derivatives as apoptosis inducers. *Med. Chem. Res.* **2022**, *31*, 368−379.
(21) Güngör, E. M.; Altıntop, M. D.; Sever, B.; Akalın Çiftçi, G. Design, synthesis, *in vitro* and *in silico* evaluation of new hydrazone-based antitumor agents as potent Akt inhibitors. *Lett. Drug Des. Discovery* **2020**, *17*, 1380−1392.
(22) Han, M.İ.; Bekçi, H.; Uba, A. I.; Yıldırım, Y.; Karasulu, E.; Cumaoğlu, A.; Karasulu, H. Y.; Yelekçi, K.; Yılmaz, Ö.; Küçükgüzel, Ş.G. Synthesis, molecular modeling, *in vivo* study, and anticancer activity of 1,2,4-triazole containing hydrazide−hydrazones derived from (*S*)-naproxen. *Arch. Pharm. Chem. Life Sci.* **2019**, *352*, No. e1800365.
(23) Viswanathan, A.; Kute, D.; Musa, A.; Konda Mani, S.; Sipilä, V.; Emmert-Streib, F.; Zubkov, F. I.; Gurbanov, A. V.; Yli-Harja, O.; Kandhavelu, M. 2-(2-(2,4-Dioxopentan-3-ylidene)hydrazineyl)-benzonitrile as novel inhibitor of receptor tyrosine kinase and PI3K/AKT/mTOR signaling pathway in glioblastoma. *Eur. J. Med. Chem.* **2019**, *166*, 291−303.
(24) Chen, X.; Li, H.; Luo, H.; Lin, Z.; Luo, W. Synthesis and evaluation of pyridoxal hydrazone and acylhydrazone compounds as potential angiogenesis inhibitors. *Pharmacology* **2019**, *104*, 244−257.
(25) Alam, M. S.; Lee, D. U. Synthesis, biological evaluation, drug-likeness, and *in silico* screening of novel benzylidene-hydrazone analogues as small molecule anticancer agents. *Arch. Pharm. Res.* **2016**, *39*, 191−201.
(26) Bak, Y.; Kim, H.; Kang, J. W.; Lee, D. H.; Kim, M. S.; Park, Y. S.; Kim, J. H.; Jung, K. Y.; Lim, Y.; Hong, J.; Yoon, D. Y. A synthetic naringenin derivative, 5-hydroxy-7,4′-diacetyloxyflavanone-N-phenyl hydrazone (N101-43), induces apoptosis through up-regulation of Fas/FasL expression and inhibition of PI3K/Akt signaling pathways in non-small-cell lung cancer cells. *J. Agric. Food Chem.* **2011**, *59*, 10286−10297.
(27) Wong, X. K.; Yeong, K. Y. A patent review on the current developments of benzoxazoles in drug discovery. *ChemMedChem* **2021**, *16*, 3237−3262.
(28) Kale, M.; Chavan, V. Exploration of the biological potential of benzoxazoles: An overview. *Mini-Rev. Org. Chem.* **2019**, *16*, 111−126.
(29) Zhang, H.-Z.; Zhao, Z.-L.; Zhou, C.-H. Recent advance in oxazole-based medicinal chemistry. *Eur. J. Med. Chem.* **2018**, *144*, 444−492.
(30) Rajasekhar, S.; Maiti, B.; Chanda, K. A decade update on benzoxazoles, a privileged scaffold in synthetic organic chemistry. *Synlett* **2017**, *28*, 521−541.
(31) Demmer, C. S.; Bunch, L. Benzoxazoles and oxazolopyridines in medicinal chemistry studies. *Eur. J. Med. Chem.* **2015**, *97*, 778−785.
(32) Taghour, M. S.; Mahdy, H. A.; Gomaa, M. H.; Aglan, A.; Eldeib, M. G.; Elwan, A.; Dahab, M. A.; Elkaeed, E. B.; Alsfouk, A. A.; Khalifa, M. M.; Eissa, I. H.; Elkady, H. Benzoxazole derivatives as new VEGFR-2 inhibitors and apoptosis inducers: Design, synthesis, *in silico* studies, and antiproliferative evaluation. *J. Enzyme Inhib. Med. Chem.* **2022**, *37*, 2063−2077.
(33) Omar, A.-M. M. E.; AboulWafa, O. M.; El-Shoukrofy, M. S.; Amr, M. E. Benzoxazole derivatives as new generation of anti-breast cancer agents. *Bioorg. Chem.* **2020**, *96*, No. 103593.
(34) Glamočlija, U.; Padhye, S.; Špirtović-Halilović, S.; Osmanović, A.; Veljović, E.; Roca, S.; Novaković, I.; Mandić, B.; Turel, I.; Kljun, J.; Trifunović, S.; Kahrović, E.; Kraljević Pavelić, S.; Harej, A.; Klobučar, M.; Završnik, D. Synthesis, biological evaluation and docking studies of benzoxazoles derived from thymoquinone. *Molecules* **2018**, *23*, No. 3297.
(35) Yaghmaei, S.; Ghalayania, P.; Salami, S.; Nourmohammadian, F.; Koohestanimobarhan, S.; Imeni, V. Hybrid benzoxazole-coumarin compounds induce death receptor-mediated switchable apoptotic and necroptotic cell death on HN-5 head and neck cancer cell line. *Anti-Cancer Agents Med. Chem.* **2017**, *17*, 608−614.
(36) Abdelgawad, M. A.; Bakr, R. B.; Omar, H. A. Design, synthesis and biological evaluation of some novel benzothiazole/benzoxazole and/or benzimidazole derivatives incorporating a pyrazole scaffold as antiproliferative agents. *Bioorg. Chem.* **2017**, *74*, 82−90.
(37) Belal, A.; Abdelgawad, M. A. New benzothiazole/benzoxazole-pyrazole hybrids with potential as COX inhibitors: design, synthesis and anticancer activity evaluation. *Res. Chem. Intermed.* **2017**, *43*, 3859−3872.
(38) An, Y.; Lee, E.; Yu, Y.; Yun, J.; Lee, M. Y.; Kang, J. S.; Kim, W.-Y.; Jeon, R. Design and synthesis of novel benzoxazole analogs as Aurora B kinase inhibitors. *Bioorg. Med. Chem. Lett.* **2016**, *26*, 3067−3072.
(39) Taskin, T.; Yilmaz, S.; Yildiz, I.; Yalcin, I.; Aki, E. Insight into eukaryotic topoisomerase II-inhibiting fused heterocyclic compounds in human cancer cell lines by molecular docking. *SAR QSAR Environ. Res.* **2012**, *23*, 345−355.
(40) Bulut, Z.; Abul, N.; Poslu, A. H.; Gülçin, İ.; Ece, A.; Erçağ, E.; Koz, Ö.; Koz, G. Structural characterization and biological evaluation of uracil-appended benzylic amines as acetylcholinesterase and carbonic anhydrase I and II inhibitors. *J. Mol. Struct.* **2023**, *1280*, No. 135047.
(41) Efeoglu, C.; Yetkin, D.; Nural, Y.; Ece, A.; Seferoğlu, Z.; Ayaz, F. Novel urea-thiourea hybrids bearing 1, 4-naphthoquinone moiety: Anti-inflammatory activity on mammalian macrophages by regulating intracellular PI3K pathway, and molecular docking study. *J. Mol. Struct.* **2022**, *1264*, No. 133284.
(42) Chan, K.; Frankish, N.; Zhang, T.; Ece, A.; Cannon, A.; O'Sullivan, J.; Sheridan, H. Bioactive indanes: insight into the bioactivity of indane dimers related to the lead anti-inflammatory molecule PH46A. *J. Pharm. Pharmacol.* **2020**, *72*, 927−937.
(43) Ece, A. Computer-aided drug design. *BMC Chem.* **2023**, *17*, No. 26.
(44) Davies, T. G.; Verdonk, M. L.; Graham, B.; Saalau-Bethell, S.; Hamlett, C. C. F.; McHardy, T.; Collins, I.; Garrett, M. D.; Workman, P.; Woodhead, S. J.; Jhoti, H.; Barford, D. A structural comparison of inhibitor binding to PKB, PKA and PKA-PKB chimera. *J. Mol. Biol.* **2007**, *367*, 882−894.
(45) Ibrahim, M.-K.; El-Adl, K.; Zayed, M. F.; Mahdy, H. A. Design, synthesis, docking, and biological evaluation of some novel 5-chloro-

https://doi.org/10.1021/acsomega.3c02331
ACS Omega 2023, 8, 20056−20065

2-substituted sulfanylbenzoxazole derivatives as anticonvulsant agents. *Med. Chem. Res.* **2015**, *24*, 99−114.
(46) Altıntop, M. D.; Sever, B.; Akalın Çiftçi, G.; Özdemir, A. Design, synthesis, and evaluation of a new series of thiazole-based anticancer agents as potent Akt inhibitors. *Molecules* **2018**, *23*, 1318.
(47) Mosmann, T. Rapid colorimetric assay for cellular growth and survival: application to proliferation and cytotoxicity assays. *J. Immunol. Methods* **1983**, *65*, 55−63.
(48) Orujova, T.; Ece, A.; Akalın Çiftçi, G.; Özdemir, A.; Altıntop, M. D. A new series of thiazole-hydrazone hybrids for Akt-targeted therapy of non-small cell lung cancer. *Drug Dev. Res.* **2023**, *84*, 185−199.
(49) *Protein Preparation Wizard*, version 2023-1; Schrödinger, LLC: New York, NY, 2023.
(50) Friesner, R. A.; Murphy, R. B.; Repasky, M. P.; Frye, L. L.; Greenwood, J. R.; Halgren, T. A.; Sanschagrin, P. C.; Mainz, D. T. Extra precision glide: Docking and scoring incorporating a model of hydrophobic enclosure for protein− ligand complexes. *J. Med. Chem.* **2006**, *49*, 6177−6196.
(51) *LigPrep*, version 2023-1; Schrödinger, LLC: New York, NY, 2023.
(52) *QikProp*, version 2023-1; Schrödinger, LLC: New York, NY, 2023.

Recommended by ACS

Design, Synthesis, and Anticancer Evaluation of Novel Tetracaine Hydrazide-Hydrazones
M. İhsan Han and Nalan İmamoğlu
FEBRUARY 28, 2023
ACS OMEGA
READ

Synthesis, Molecular Docking, and Biological Evaluation of a New Series of Benzothiazinones and Their Benzothiazinyl Acetate Derivatives as Anticancer Agents against MCF-7...
Farhat Ramzan, Kalim Javed, *et al.*
FEBRUARY 07, 2023
ACS OMEGA
READ

Terminators or Guardians? Design, Synthesis, and Cytotoxicity Profiling of Chalcone-Sulfonamide Hybrids
Shaimaa M. Aboukhatwa, Haytham O. Tawfik, *et al.*
FEBRUARY 17, 2023
ACS OMEGA
READ

Evaluation of In Vivo Biological Activity Profiles of Isoindole-1,3-dione Derivatives: Cytotoxicity, Toxicology, and Histopathology Studies
Aytekin Köse, Gülşah Şanlı-Mohamed, *et al.*
MARCH 21, 2023
ACS OMEGA
READ

Get More Suggestions >

https://doi.org/10.1021/acsomega.3c02331
ACS Omega 2023, 8, 20056−20065